SUPPORTING INFORMATION

Comparison of *Drosophila melanogaster* embryo and adult proteome by SWATH-MS reveals differential regulation of protein synthesis, degradation machinery and metabolism modules

Bertrand Fabre[1,2,4,5,†,*], Dagmara Korona[3,4,†], Jonathan G. Lees[6], Ikrame Lazar[5], Ido Livneh[5], Manon Brunet[1,2,4], Christine A. Orengo[6], Steven Russell[3,4], Kathryn S. Lilley[1,2,4,*]

1. Cambridge Centre for Proteomics, Department of Biochemistry, University of Cambridge, Cambridge, U.K

2. Department of Biochemistry, University of Cambridge, University of Cambridge, Cambridge, U.K

3. Department of Genetics, University of Cambridge, University of Cambridge, Cambridge, U.K

4. Cambridge Systems Biology Centre, University of Cambridge, Cambridge, U.K

5. Technion Integrated Cancer Center (TICC), The Rappaport Faculty of Medicine and Research Institute, Haifa, Israel

6. Institute of Structural and Molecular Biology, University College London, London, United Kingdom

† These authors contributed equally to this work.

* Correspondence:

Pr. Kathryn S. Lilley, Ph.D., Cambridge Centre for Proteomics, Cambridge Systems Biology Centre, Department of Biochemistry, University of Cambridge, Cambridge CB2 1QR, U.K. Telephone: 01223 760255; e-mail: k.s.lilley@bioc.cam.ac.uk

Dr. Bertrand Fabre, Ph.D., Technion Integrated Cancer Center (TICC), The Rappaport Faculty of Medicine and Research Institute, Haifa, Israel, e-mail: bertrand.fabre@cantab.net

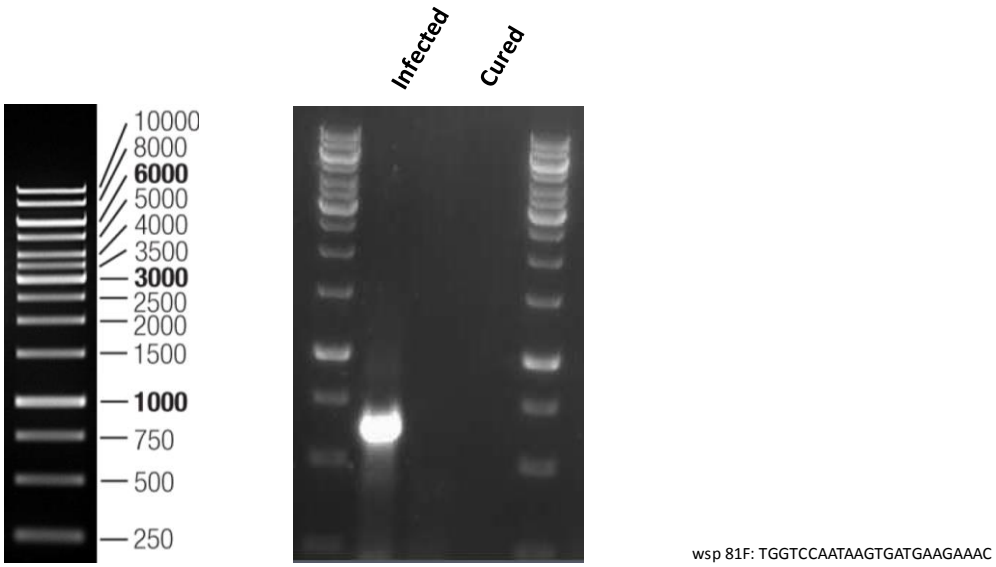

632 bp fragment of the Wolbachia Surface Protein gene (genbank accession no: EU395833.1).

Figure S1: Verification of Wolbachia infection status of fly lines by PCR

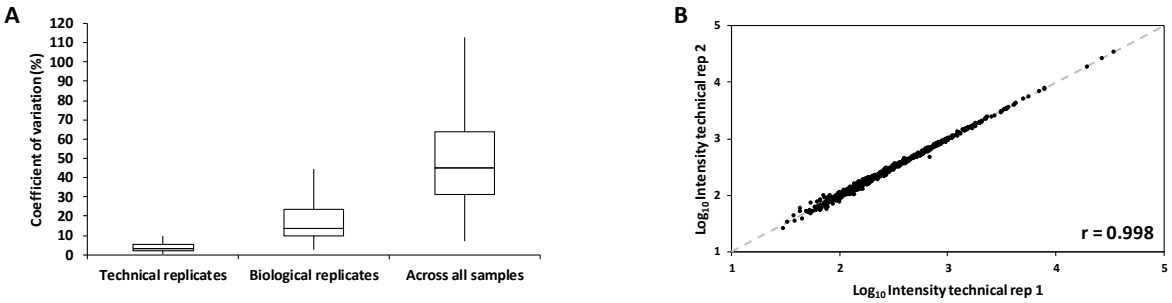

C

	Technical rep 1	Technical rep 2	Technical rep 3	Technical rep 4
Technical rep 1		0.998	0.998	0.997
Technical rep 2			0.998	0.997
Technical rep 3				0.997
Technical rep 4				

Figure S2: Reproducibility of the SWATH-MS workflow

A. Coefficients of variation were calculated for each protein quantified between technical (injection), biological replicates or across all the samples. B. Pairwise comparison between two technical (injection) replicates. Pearson coefficient of correlation is indicated on the graph. C. Pearson coefficient of correlation calculated from pairwise comparison of 4 technical (injection) replicates.

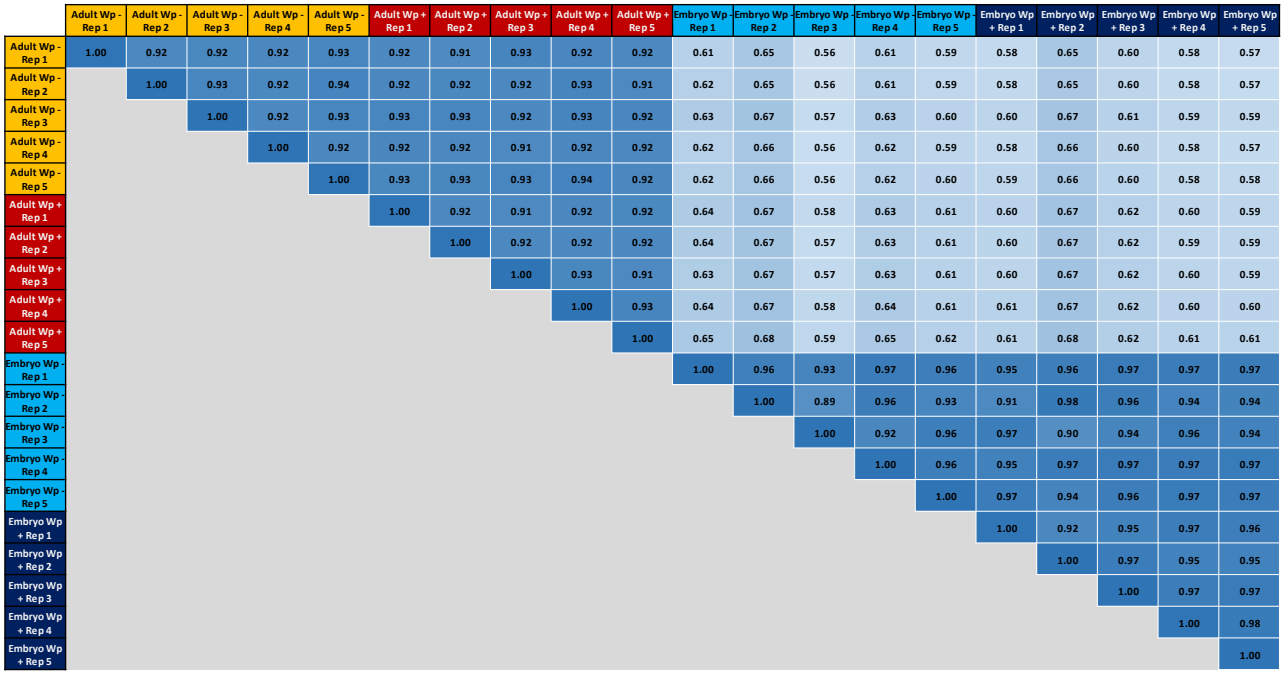

	Adult Wp - Rep 1	Adult Wp - Rep 2	Adult Wp - Rep 3	Adult Wp - Rep 4	Adult Wp - Rep 5	Adult Wp + Rep 1	Adult Wp + Rep 2	Adult Wp + Rep 3	Adult Wp + Rep 4	Adult Wp + Rep 5	Embryo Wp - Rep 1	Embryo Wp - Rep 2	Embryo Wp - Rep 3	Embryo Wp - Rep 4	Embryo Wp - Rep 5	Embryo Wp + Rep 1	Embryo Wp + Rep 2	Embryo Wp + Rep 3	Embryo Wp + Rep 4	Embryo Wp + Rep 5
Adult Wp - Rep 1	1.00	0.92	0.92	0.92	0.93	0.92	0.91	0.93	0.92	0.92	0.61	0.65	0.56	0.61	0.59	0.58	0.65	0.60	0.58	0.57
Adult Wp - Rep 2		1.00	0.93	0.92	0.94	0.92	0.92	0.92	0.93	0.91	0.62	0.65	0.56	0.61	0.59	0.58	0.65	0.60	0.58	0.57
Adult Wp - Rep 3			1.00	0.92	0.93	0.93	0.93	0.92	0.93	0.92	0.63	0.67	0.57	0.63	0.60	0.60	0.67	0.61	0.59	0.59
Adult Wp - Rep 4				1.00	0.92	0.92	0.92	0.91	0.92	0.92	0.62	0.66	0.56	0.62	0.59	0.58	0.66	0.60	0.58	0.57
Adult Wp - Rep 5					1.00	0.93	0.93	0.93	0.94	0.92	0.62	0.66	0.56	0.62	0.60	0.59	0.66	0.60	0.58	0.58
Adult Wp + Rep 1						1.00	0.92	0.91	0.92	0.92	0.64	0.67	0.58	0.63	0.61	0.60	0.67	0.62	0.60	0.59
Adult Wp + Rep 2							1.00	0.92	0.92	0.92	0.64	0.67	0.57	0.63	0.61	0.60	0.67	0.62	0.59	0.59
Adult Wp + Rep 3								1.00	0.93	0.91	0.63	0.67	0.57	0.63	0.61	0.60	0.67	0.62	0.60	0.59
Adult Wp + Rep 4									1.00	0.93	0.64	0.67	0.58	0.64	0.61	0.61	0.67	0.62	0.60	0.60
Adult Wp + Rep 5										1.00	0.65	0.68	0.59	0.65	0.62	0.61	0.68	0.62	0.61	0.61
Embryo Wp - Rep 1											1.00	0.96	0.93	0.97	0.96	0.95	0.96	0.97	0.97	0.97
Embryo Wp - Rep 2												1.00	0.89	0.96	0.93	0.91	0.98	0.96	0.94	0.94
Embryo Wp - Rep 3													1.00	0.92	0.96	0.97	0.90	0.94	0.96	0.94
Embryo Wp - Rep 4														1.00	0.96	0.95	0.97	0.97	0.97	0.97
Embryo Wp - Rep 5															1.00	0.97	0.94	0.96	0.97	0.97
Embryo Wp + Rep 1																1.00	0.92	0.95	0.97	0.96
Embryo Wp + Rep 2																	1.00	0.97	0.95	0.95
Embryo Wp + Rep 3																		1.00	0.97	0.97
Embryo Wp + Rep 4																			1.00	0.98
Embryo Wp + Rep 5																				1.00

Figure S3: Pearson coefficient of correlation calculated between all the samples from pairwise comparison.

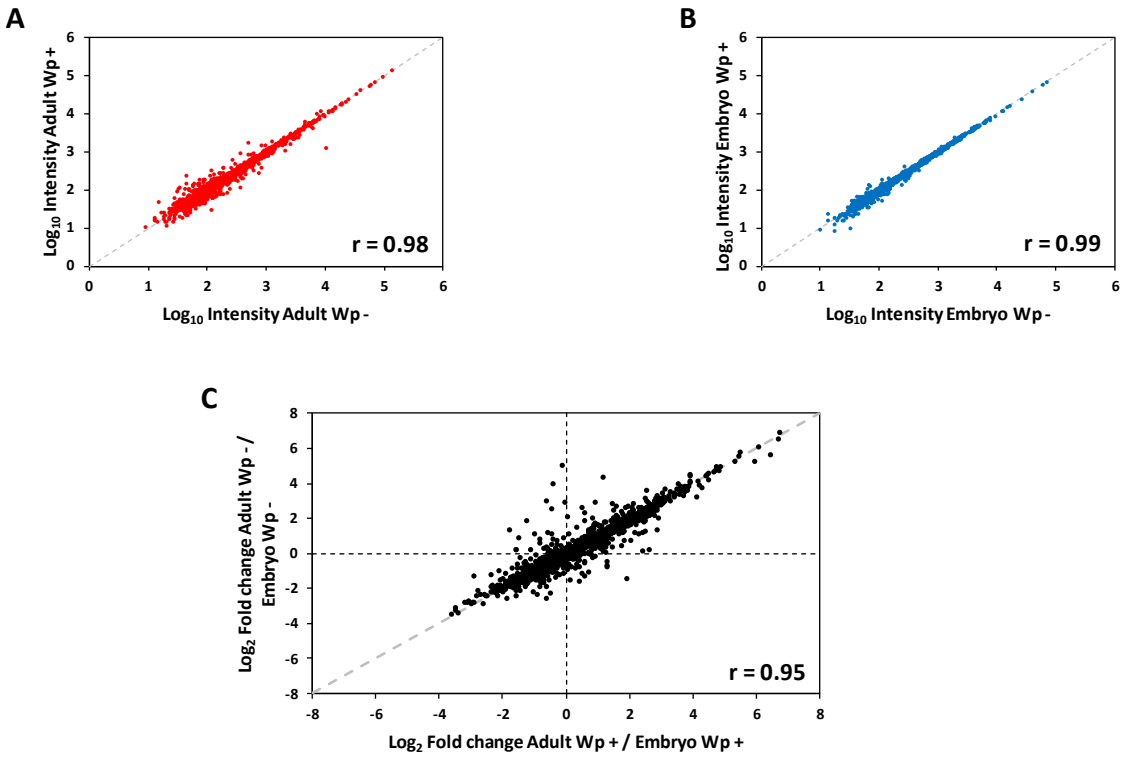

Figure S4: Comparison of Wolbachia infected and cured samples

A-B. Comparison of average protein intensities between Wolbachia infected (Wp+) and cured (Wp-) adult fly (A) and embryo (B). Pearson coefficient of correlation is indicated on the graphs.

C. Comparison of the average ratio adult/embryo protein intensities between Wolbachia infected (Wp+) and cured (Wp-) adult fly (A) and embryo (B) infected with Wolbachia (Wp+) and cured (Wp-). Pearson coefficient of correlation is indicated on the graph.

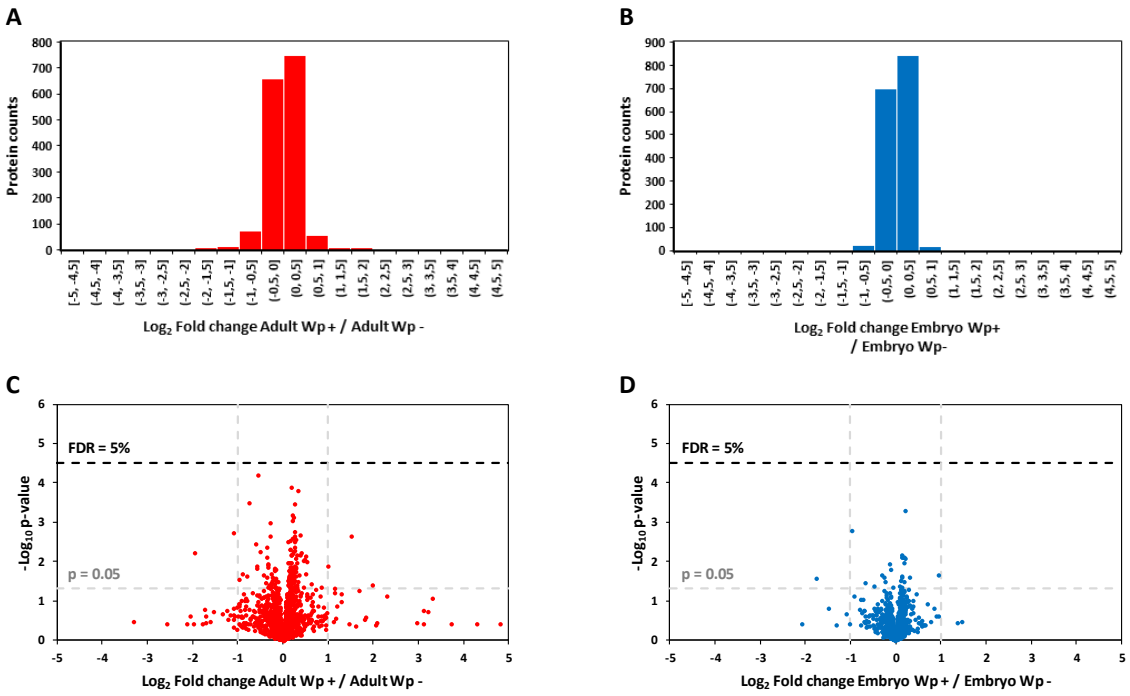

Figure S5: Effect of *Wolbachia pipientis* on the embryo and adult fly proteomes

A-B. Graphs representing the distribution of $\log_2$ ratio Wolbachia infected (Wp+) / cured (Wp-) for adult fly (A) and embryo (B). C-D. Volcano plot representing the $\log_2$ ratio Wolbachia infected (Wp+) / cured (Wp-) for adult fly (C) and embryo (D) and the corresponding Benjamini-Hochberg corrected p-value. Dashed lines represent the thresholds for $\log_2$ fold change of 1 and -1 as well as p-value of 0.05 and FDR of 5%.

Figure S6A

Aconitate (Q9VIE8_DROME) Spectronaut average measured Adult/Embryo ratio : 11.4

WVAVGDENYGEGSSR

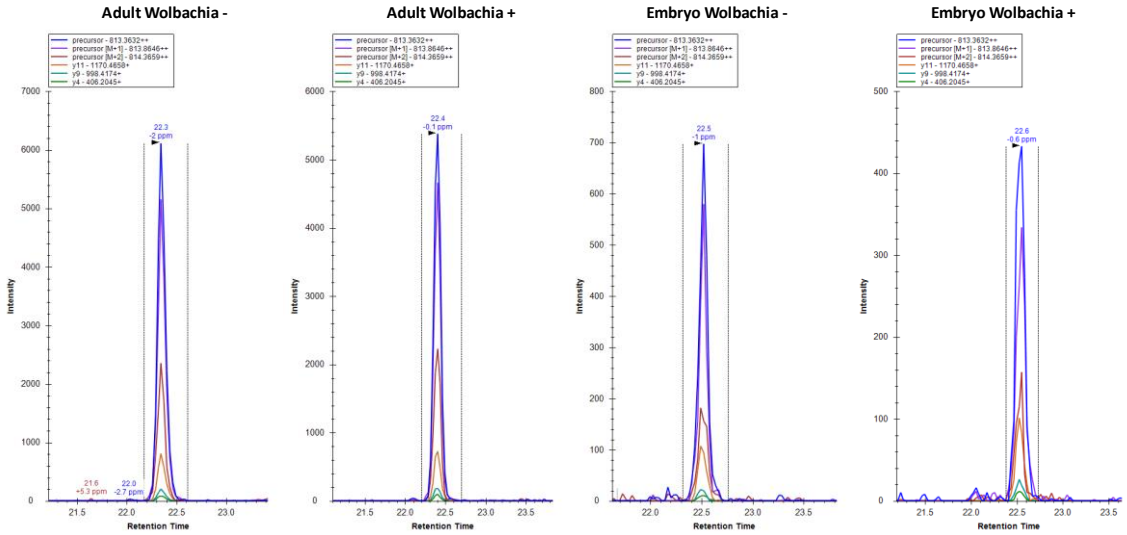

Figure S6B

ATP synthase subunit alpha (Protein bellwether)(ATPA_DROME) Spectronaut average measured Adult/Embryo ratio : 5.8

QGQYVPMAIEDQVAVIYCGVR

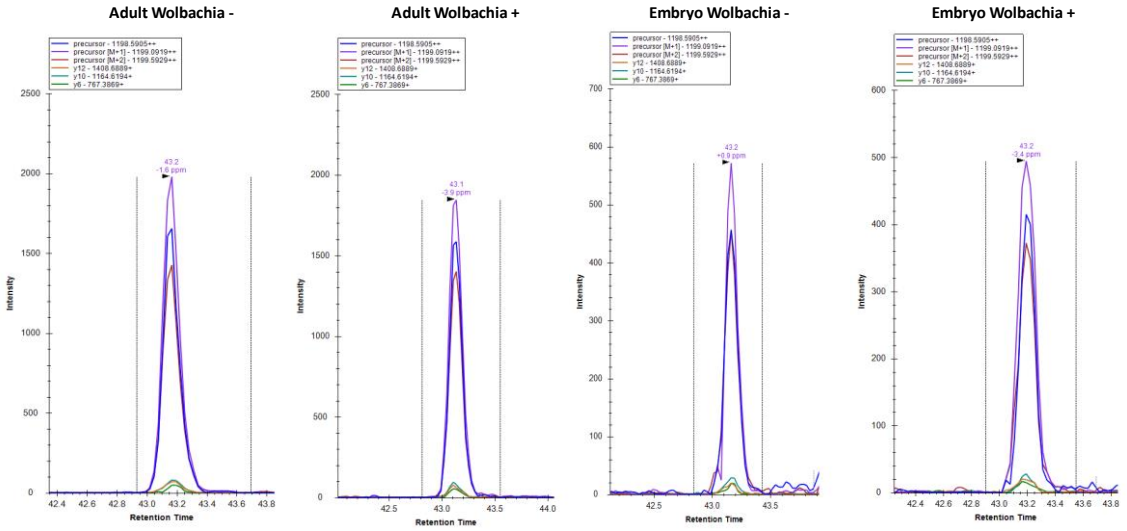

Figure S6C

Proteasome subunit alpha type-1 (PSA1_DROME) Spectronaut average measured Adult/Embryo ratio : 0.33

HSYDTTYPVSR

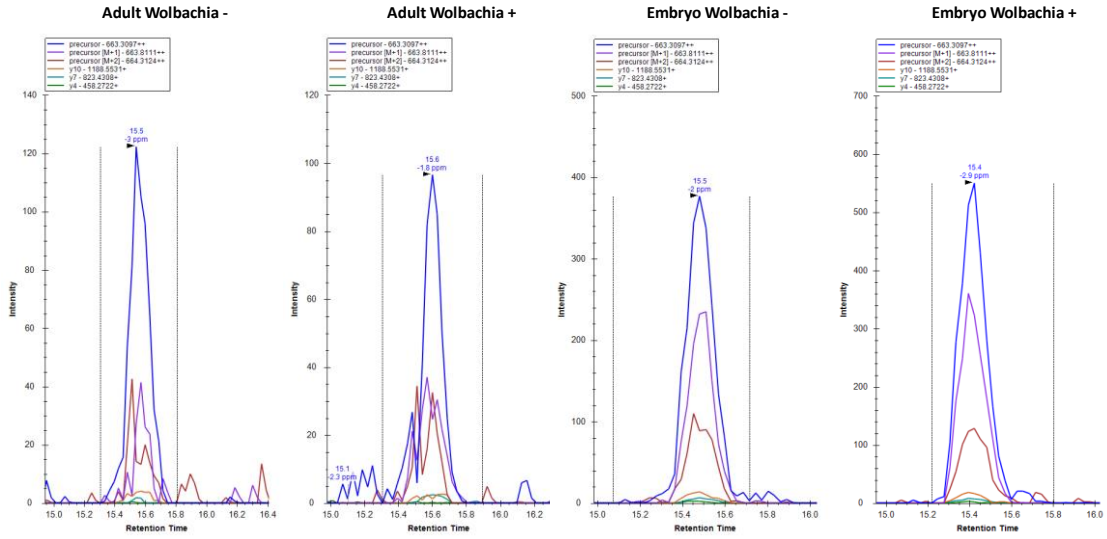

Figure S6D

60S ribosomal protein L4 (RL4_DROME) Spectronaut average measured Adult/Embryo ratio : 0.38

FVIWTESAFAR

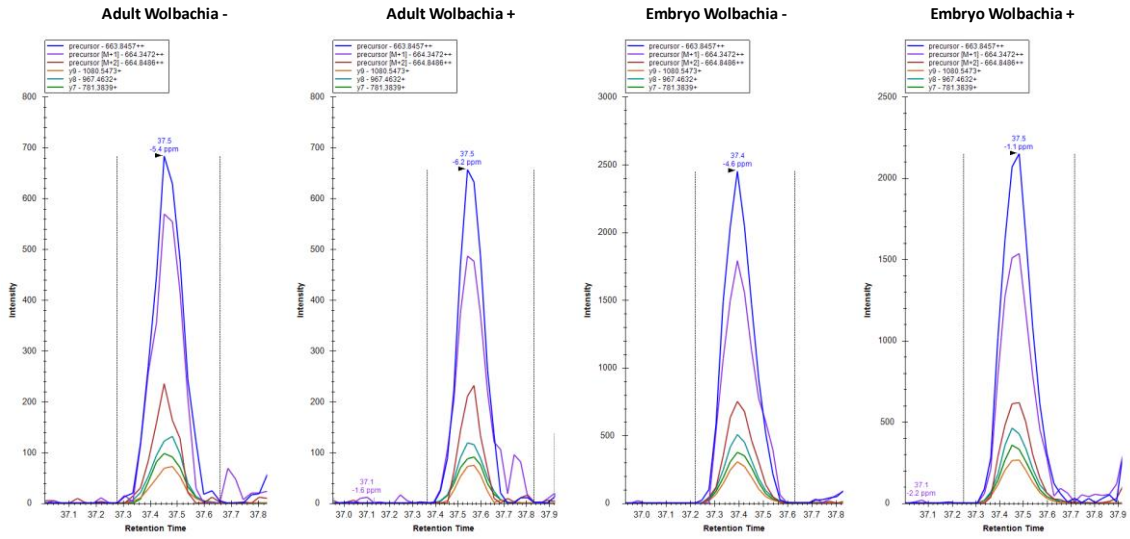

Figure S6: Skyline validation of the SWATH-MS data

A-D. Extracted ion chromatograms from the re-analysis of the data using Skyline are presented for peptides of Aconitate (A), ATP synthase subunit alpha (Protein bellwether) (B), Proteasome subunit alpha type-1 (C) and 60S ribosomal protein L4 (D). The adult/embryo ratio measured using Spectronaut is given for each protein.

Figure S7A

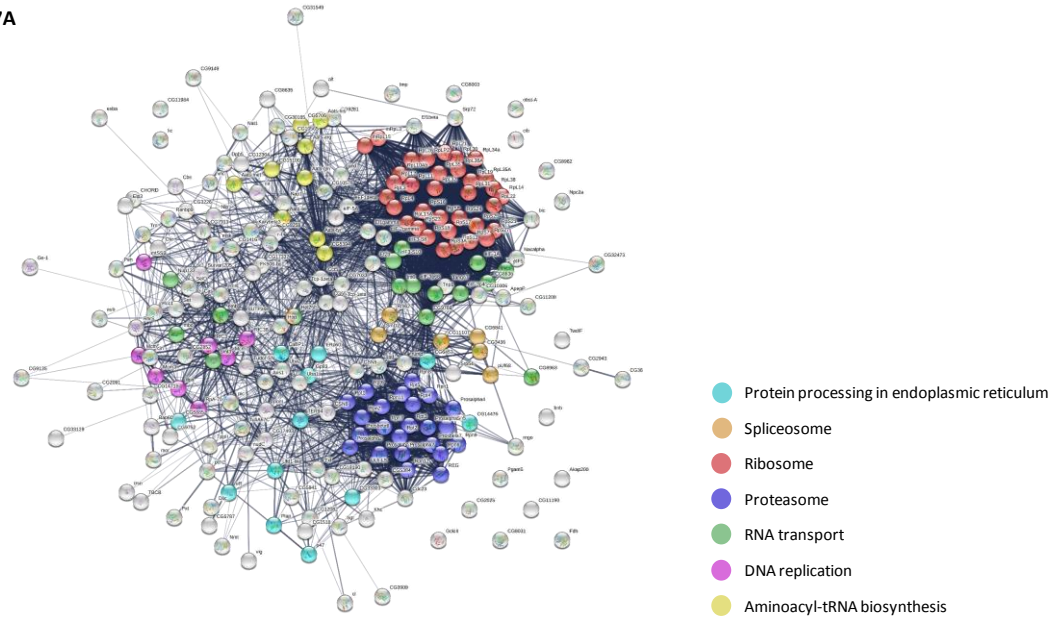

Figure S7B

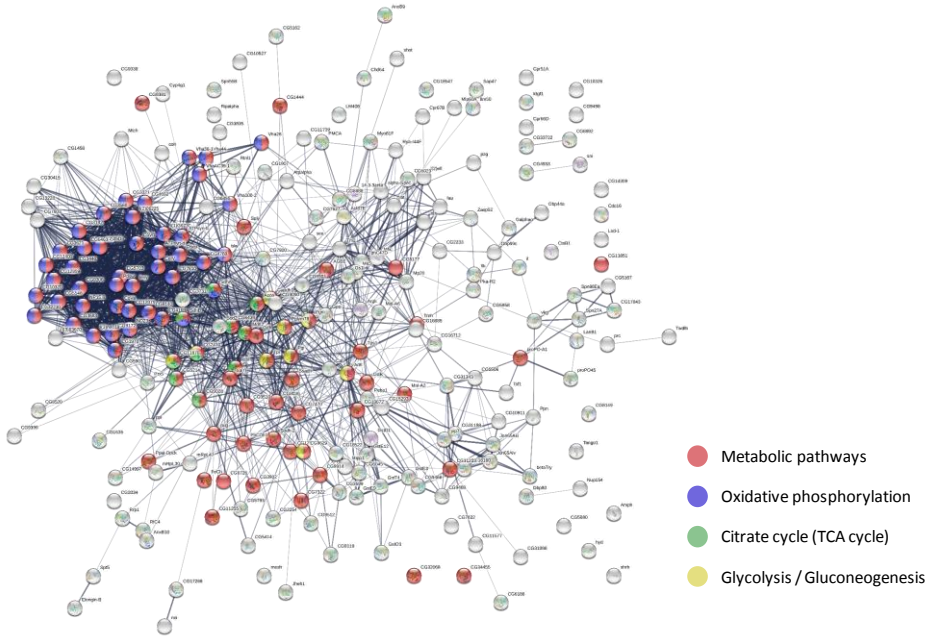

Figure S7: Network representation of differentially regulated proteins between adult fly and embryo

A-B. Graph representing the STRING analysis of the proteins more abundant in embryo (A) and adult flies (B). Proteins belonging to significantly enriched pathways are highlighted.

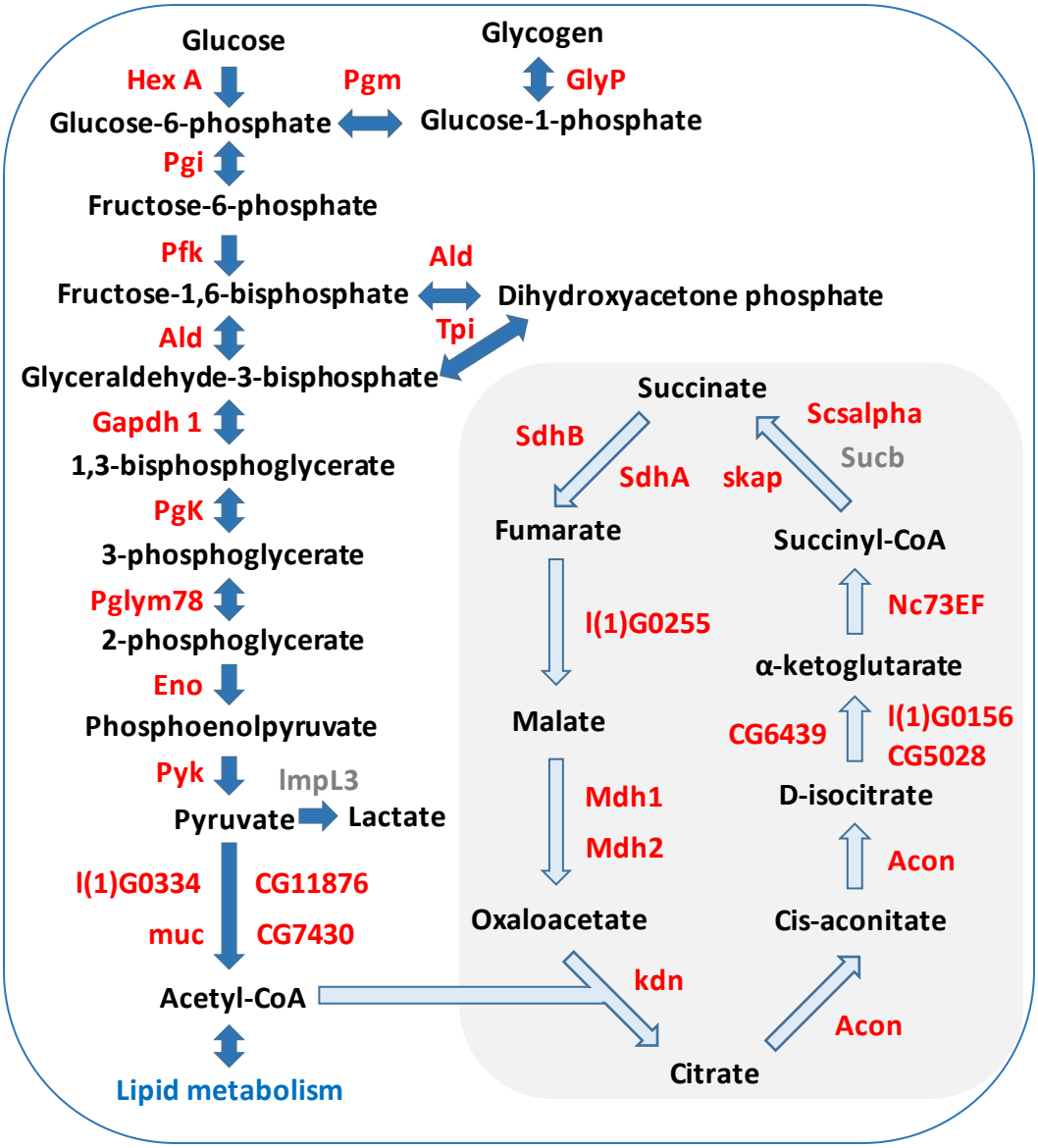

Figure S8: Proteins from glycolysis and TCA cycle are more abundant in adult fly compared to embryo

Graph displaying the enzymes involved in glycolysis and TCA cycle. Enzymes with name in blue, red and grey represent proteins more abundant in embryo, in adult flies and not significantly changing, respectively.

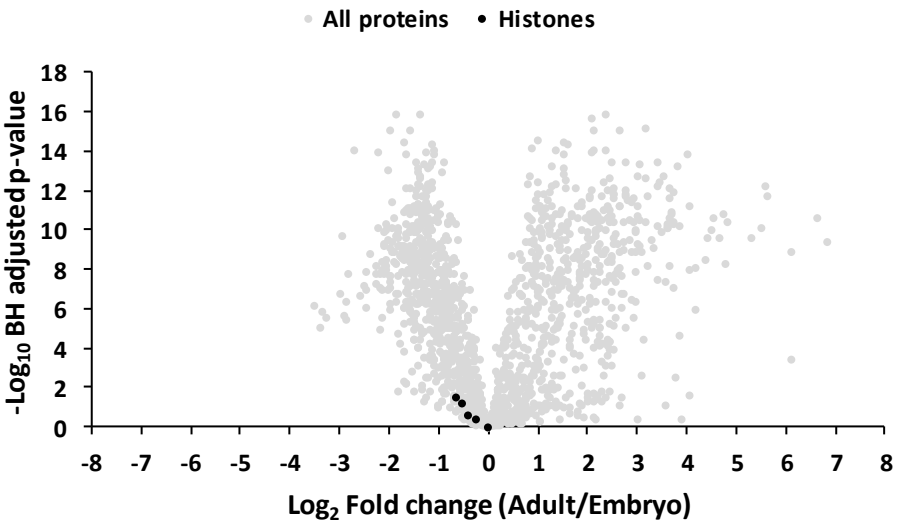

Figure S9: Histones remain constant between embryo and adult fly

Volcano plot representing the $\log_2$ ratio (adult/embryo) for each protein quantified and the corresponding Benjamini-Hochberg corrected p-value. Histones are represented of the graphs.

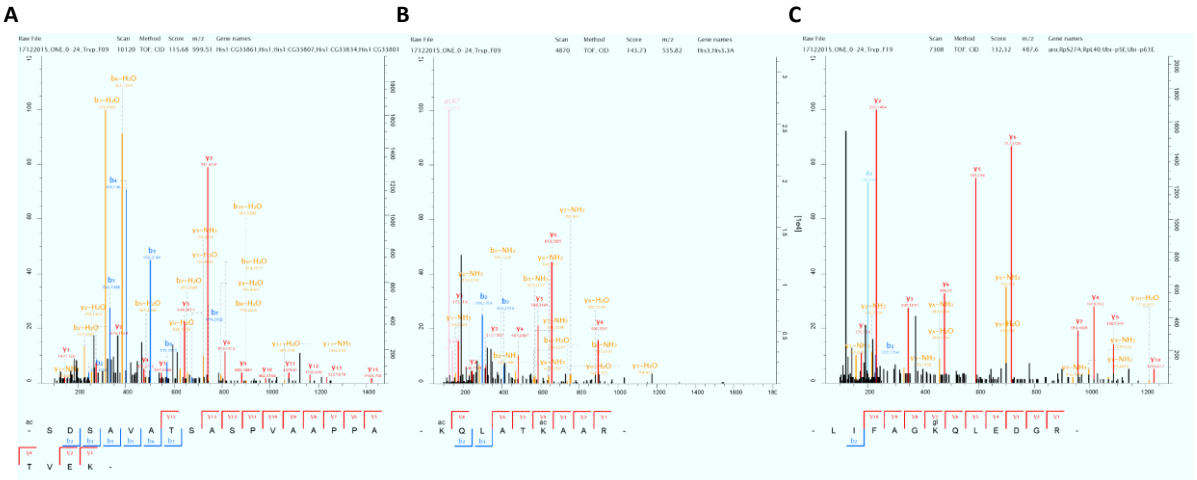

Figure S10: MSMS spectra for acetylated histones and K48 ubiquitin linkage

A-C. MSMS spectra of the acetylated peptide acSDSAVATSASPVAAPPATVEK of the histone H1 (A), the acetylated peptide acKQLATacKAAR of the histone H3 (B) and the peptide reporting K48 ubiquitin linkage LIFAGK[GG]QLEDGR (C) identified in the spectral library using MaxQuant.

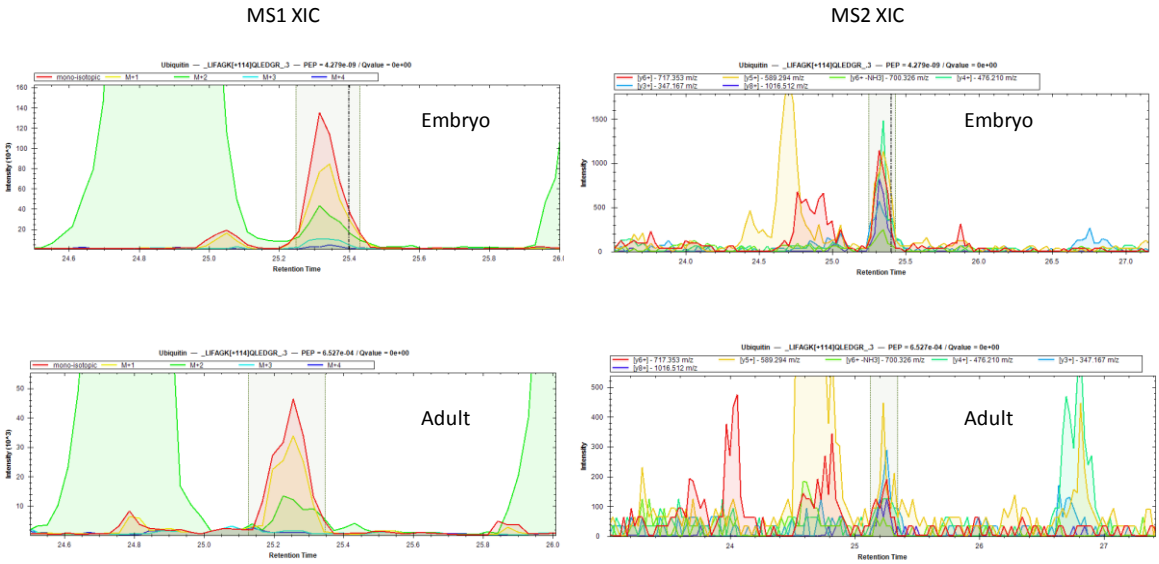

Figure S11: Extracted ion chromatograms of the peptide reporting K48 ubiquitin linkage LIFAGK[GG]QLEDGR

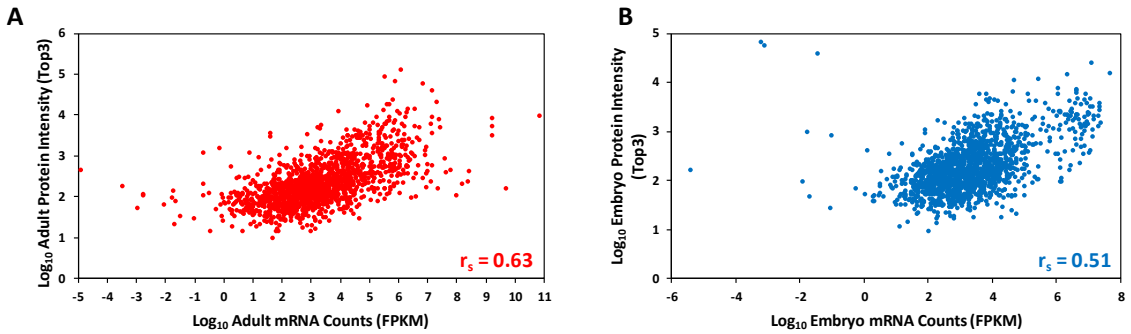

Figure S12: Protein/mRNA correlation in adult fly and embryo

A-B. Graphs representing the $\log_{10}$ protein intensities (calculated using the Top3 method) against the adult $\log_{10}$ mRNA counts (calculated using the modENCODE data) for adult fly (A) and embryo (B). The resulting Spearman's rank correlation coefficients are indicated on the graphs.

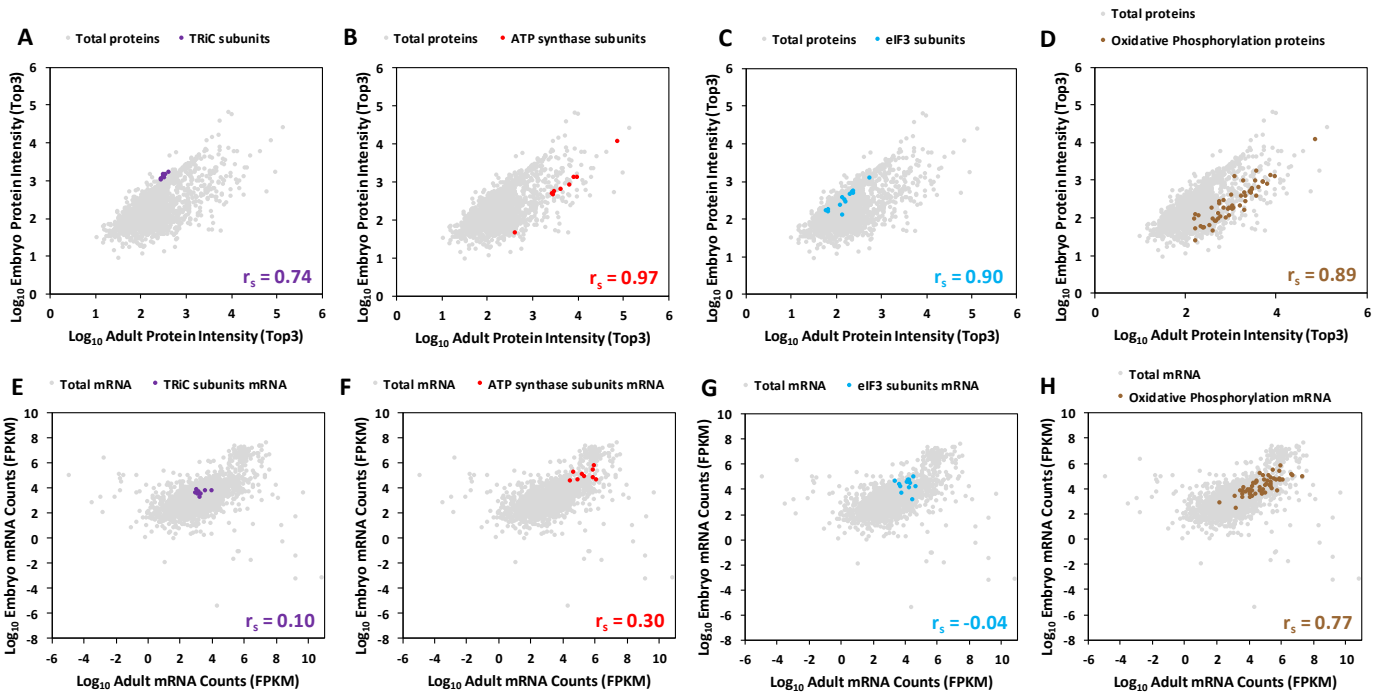

Figure S13: Correlation of Protein and mRNA components of modules

A-D. Graph representing the embryo $\log_{10}$ protein intensities (calculated using the Top3 method) against the adult $\log_{10}$ protein intensities. TRiC (A), ATP synthase (B), eIF3 (C) and Oxidative phosphorylation (D) components proteins intensities are represented on the graphs. E-H. Graph representing the embryo $\log_{10}$ mRNA counts (calculated using the modENCODE data) against the adult $\log_{10}$ mRNA counts. TRiC (E), ATP synthase (F), eIF3 (G) and Oxidative phosphorylation (H) components mRNA counts are represented on the graphs. The resulting Spearman's rank correlation coefficient is indicated on the graphs.

Figure S14A

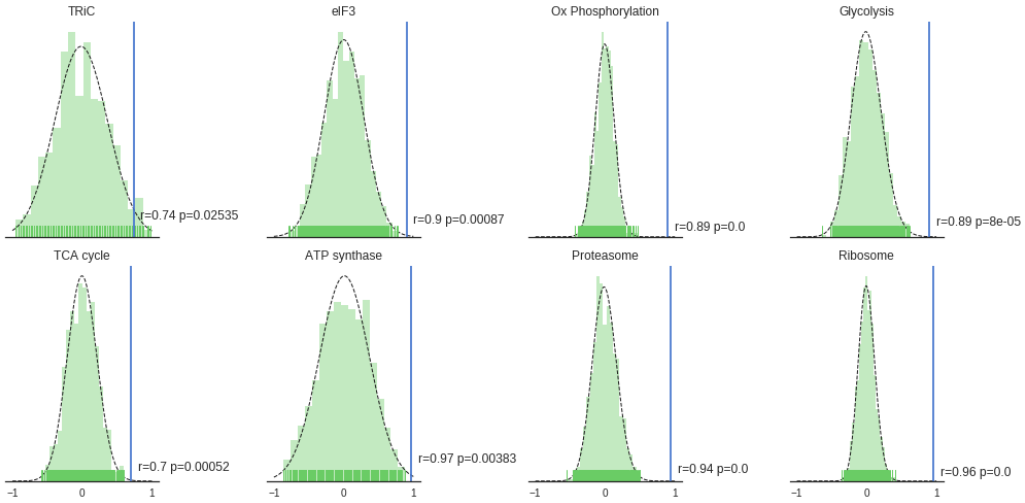

Figure S14B

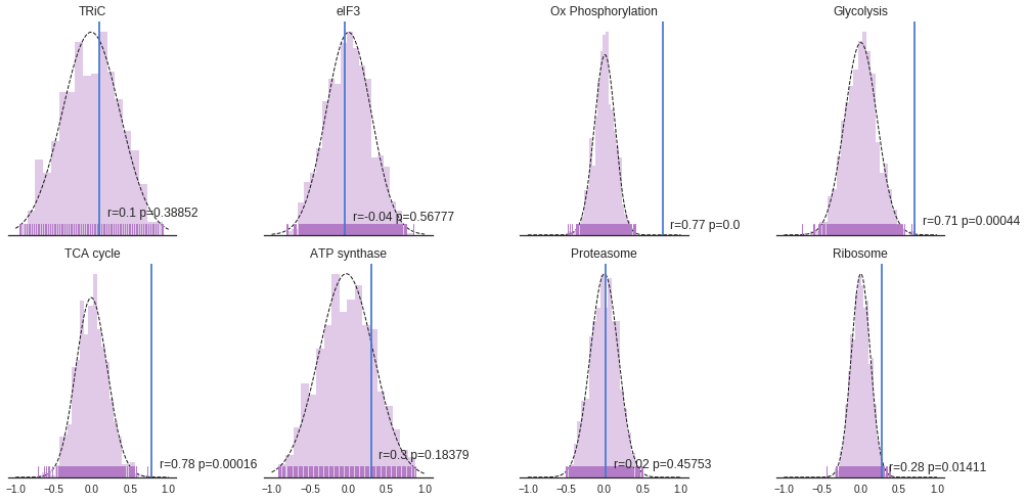

Figure S14: Random sampling experiments with the sample size matching the number of genes quantified in each protein module

A-B. Graph representing the skew-normal distribution fitted to the Spearman's rank correlation coefficient distribution of 1,000 random samples at the protein (A) and mRNA (B) level. The corresponding p-value was estimated for each protein module.

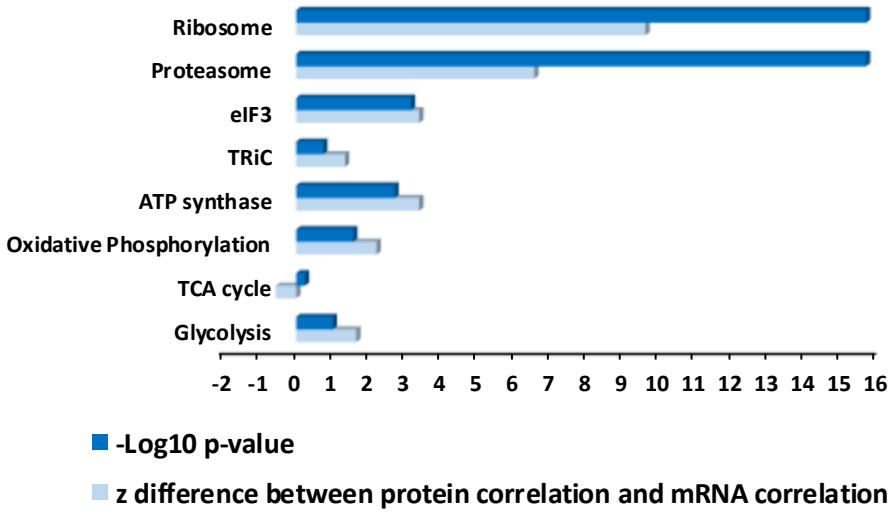

Figure S15: Differences between Protein and mRNA components of modules correlation

Coefficient of correlations observed at the protein and mRNA level for these protein modules were transformed using Fisher r-to-z transformation to assess the difference between the correlations. A graph representing the z differences and the corresponding $-\log_{10}$ p-values for the different protein modules is displayed.

Table S1. Table containing the SWATH-MS data

Table S2. Table containing the protein and mRNA data

Table S3. Table containing the post-translational modifications data